Scientific Research Publishing

International Journal of Modern Nonlinear Theory and Application, 2026, 15(1), 1-16
https://www.scirp.org/journal/ijmnta
ISSN Online: 2167-9487
ISSN Print: 2167-9479

Experimental Study of the Dynamic Response of the Vilnius Oscillator Based on the Resistance Connected to the Non-Inverting Input of the Operational Amplifier

Joel Calin Nkouagnou, René Kouayep Mboyo

Department of Mechatronics, Higher Institute of Transport, Logistics and Commerce, University of Ebolowa, Ebolowa, Cameroon
Email: calinjoel915@gmail.com

How to cite this paper: Nkouagnou, J.C. and Mboyo, R.K. (2026) Experimental Study of the Dynamic Response of the Vilnius Oscillator Based on the Resistance Connected to the Non-Inverting Input of the Operational Amplifier. *International Journal of Modern Nonlinear Theory and Application*, **15**, 1-16.
https://doi.org/10.4236/ijmnta.2026.151001

Received: February 18, 2026
Accepted: March 24, 2026
Published: March 27, 2026

Abstract

This work focuses on the theoretical and experimental study of the dynamic behavior of the Vilnius electronic oscillator. The theoretical study involves modeling the system using a set of three first-order differential equations and performing its numerical analysis for different values of the circuit components. The experimental study is carried out using electronic components with a control parameter. It is demonstrated that, depending on the value of the resistance connected to the non-inverting input of the operational amplifier, the Vilnius oscillator can exhibit different behaviors and generate various types of dynamics, including harmonic oscillations and chaos. This result is supported by a bifurcation diagram and the Lyapunov exponent curve. The numerical and experimental results show good qualitative agreement.

Keywords

Bifurcations, Chaos, Lyapunov Exponents, Vilnius Oscillator, Modeling

1. Introduction

To function, natural or industrial systems require specific signals to provide a useful response. For example, to produce a frequency-modulated signal, a harmonic oscillator capable of performing this modulation is needed. Recently, interest in using chaotic signals in industrial applications and communications has increased, particularly for chaotic masking in telecommunications [1] [2], power generators and industrial sieving [3].

To generate chaotic signals, for the above applications, we need electronic

circuits that are able to provide them. In [4], some of the most famous chaos circuit such as Chua's, Colpitts and Wien-brige are listed. Van der pol oscillator presented in [5] is also used to generate chaotic oscillations which are used to secure communication.

In 2004, Vilnius chaotic oscillator was proposed for the first time by the team of semiconductor Physics researchers of the physics Institute of Vilnius University [6]. The Vilnius circuit has the advantage of being very simple and easy to realize according to the type of its components. The non-linearity of the circuit is due to the diode in parallel with the capacitor at the output of the operational amplifier.

Originally, the Vilnius system was intended for educational purposes, but it quickly aroused considerable interest among many researchers. From this perspective, in [7], The authors demonstrated, through the bifurcation diagram, that the Vilnius oscillator can exhibit different types of dynamic behavior, such as harmonic oscillations as well as chaotic oscillations, depending on the system parameters, [8] used Vilinus chaotic oscillator in digital commucation and demonstrated that it is advantageous to use chaotic waveforms for the Internet of Things communication systems because chaotic communication systems shows a good resistant to channels with selective degradation and in the case of disturbances as noise.

According to the previous work on the Vilnius oscillator, all the authors [6]-[9] assumed that the excitation current was constant, with a constraint on the value of the resistance in series with the generator. However, the electrical potential at the common node of the branches containing the coil, capacitors, diode, and generator is not constant, given the electrical phenomena occurring there, it becomes interesting to obtain a new mathematical model of the system without resorting to this approximation, then to analyze the system's dynamic response, both theoretically and experimentally, and to compare the obtained results with the previous one in view to potential applications.

This paper is structured as follows: in Section 2, the problem statement is presented. The schematic and mathematical modeling of the Vilnius oscillator is the subject of section 3. In Section 4, the stability of the system is analyzed, and in section 5 the numerical results of the system dynamics are presented. The experimental study and its results are described in section 6, and section 7 concludes the paper.

2. Problem Statement

The first mathematical model of the Vilnius oscillator was obtained by considering the excitation current as constant, an approach adopted by other researchers [6]-[10]. The aim of this work is to obtain a new mathematical model of the Vilnius oscillator by considering the excitation current as a variable due to the oscillator's electrical structure, and to study its dynamic response using numerical and experimental approaches in order to compare the results with the first model of Vilnius oscillator.

3. Dynamic Model of Vilnius Oscillator

As announced in the introduction, the structure of the Vilnius oscillator is very simple given the number and the type of its components (**Figure 1**). In this work, we consider equations expanded in [6] with the difference that the current through resistor R_4 is not constant as considered in [6]-[8]. The aim here is to know if by considering that the excitation current is constant, this doesn't have a significant influence on the dynamic response of the system. In fact, the considered current is established in the circuit due to the electric potential difference between the potential V_b and V_N. With the above consideration coupled to Kirchhoff's laws, the new mathematical model of Vilnius chaotic oscillator is obtained as follows: The current through the capacitor C_1 and inductor L is given by Eq. (3.1).

$$C_1 \frac{\mathrm{d}V_{C1}}{\mathrm{d}t} = I_L \tag{3.1}$$

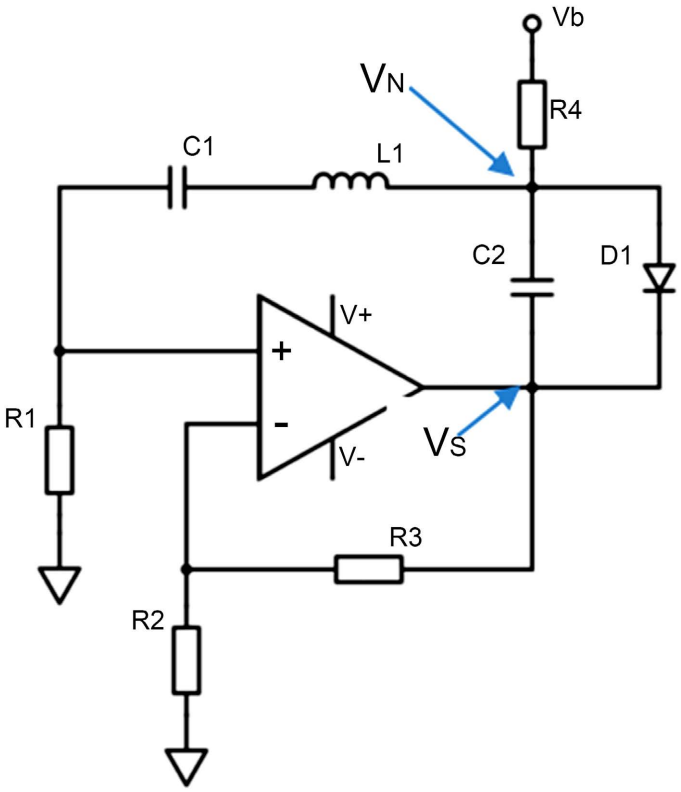

Figure 1. Vilnius oscillator schematic.

Between the ground and potential V_N, the relationship between the voltages across resistor R_1, inductor L_1 and capacitor C_1 is given by Eq.(3.2).

$$L \frac{\mathrm{d}I_L}{\mathrm{d}t} = V_N - V_{C1} - R_1 I_L \tag{3.2}$$

Considering the branch between V_b and V_N, current I is given by the following relation from the ohm's law.

$$I = \frac{V_b - V_N}{R_4} \tag{3.3}$$

In the previous model, the authors considered $I \approx \frac{V_b}{R_4}$ with V_b a constant voltage delivered by a given battery. Normaly, to be strict about the electrical phenomenon at node *N*, when the circuit oscillates, the electrical potential V_N varies due to the variations of the voltages across the inductor and the capacitor C_2. V_N then takes the form of Eq.(3.4).

$$V_N = V_S + V_{C2} \tag{3.4}$$

According to Eqs.(3.3) and (3.4), it is clear that the excitation current I is not cinstant. Based on the fact that for a given perfect operational amplifier, the following relation $V_+ = V_-$ is considered, and used to establish that $V_S = kR_1 I_L$ then Eq.(3.2) become Eq. (3.5) below:

$$L_1 \frac{\mathrm{d}I_L}{\mathrm{d}t} = (k-1) R_1 I_L - V_{C2} - V_{C1}. \tag{3.5}$$

The law of nodes in N is written as follows:

$$C_2 \frac{\mathrm{d}V_{C2}}{\mathrm{d}t} = I + I_L - I_D. \tag{3.6}$$

By combining Eq.(3.3) and Eq(3.4), Eq.(3.6) become the following equation.

$$C_2 \frac{\mathrm{d}V_{C2}}{\mathrm{d}t} = \frac{V_b}{R_4} - \frac{V_{C2}}{R_4} + \left(1 - k\frac{R_1}{R_4}\right) I_L - I_D \tag{3.7}$$

$$\begin{cases} C_1 \dfrac{\mathrm{d}V_{C1}}{\mathrm{d}t} = I_L \\ L \dfrac{\mathrm{d}I_L}{\mathrm{d}t} = (k-1) R_1 I_L - V_{C1} - V_{C2} \\ C_2 \dfrac{\mathrm{d}V_{C2}}{\mathrm{d}t} = \dfrac{V_b}{R_4} - \dfrac{V_{C2}}{R_4} + \left(1 - k\dfrac{R_1}{R_4}\right) I_L - I_D \end{cases} \tag{3.8}$$

Finally, the new model of vilnius oscillator is given by Eq.(3.8) which is a system of three first-order differential equations where C_1 and C_2 are the capacitors whose voltages across them are V_{C1} and V_{C2} respectively, I_L is the current flowing through the coil L, k is the gain of the operational amplifier, I_D is the current of the diode D_1.

$$k = 1 + \frac{R_3}{R_2} \tag{3.9}$$

$$I_D = I_S \left(\exp\left(\frac{eV_{C2}}{k_B T} \right) - 1 \right) \tag{3.10}$$

with I_S the reverse saturation current, e the electron charge, k_B the Boltzmann constant and T the temperature [9]. According to the expression of I_D ,the nonlinearity in Eq.(3.8) is due to the diode D_1 in the Vilnius electronic circuit.

In goal to facilitate the numerical analysis of the system Eq.(3.8), dimensionless variables were proposed by [6] and improved as indicated in Eq.(3.11) and Eq.(3.12a) where t is time.

$$\begin{aligned} &x=\frac{V_{C1}}{V_0}, z=\frac{V_{C2}}{V_0}, y=\frac{I_L}{w_0 C_1 V_0}, a=(k-1)R_1\sqrt{\frac{C_1}{L}}, a_1=\frac{\sqrt{LC_1}}{R_4 C_2},\\ &a_2=\left(1+\frac{kR_1}{R_4}\right)*beta, c=\frac{I_s\sqrt{LC_1}}{C_2 V_0}, u=\frac{V_{CC}\sqrt{LC_1}}{R_4 V_0 C_2}, k=1+\frac{R_3}{R_2},\\ &beta=\frac{C_1}{C_2}, V_0=\frac{k_B T}{e}, \tau=w_0 t \text{ and } w_0=\frac{1}{\sqrt{LC_1}} \end{aligned} \tag{3.11}$$

with consider variables and parameters, Eq.(3.8) become Eq. (3.12a) below.

$$\begin{cases} \dfrac{\mathrm{d}x}{\mathrm{d}\tau}=y \\ \dfrac{\mathrm{d}y}{\mathrm{d}\tau}=ay-x-z \\ \dfrac{\mathrm{d}z}{\mathrm{d}\tau}=u-a_1 z+a_2 y-c\left(\exp(z)-1\right) \end{cases} \tag{3.12a}$$

$$\begin{cases} C_1\dfrac{\mathrm{d}V_{C1}}{\mathrm{d}t}=I_L \\ L\dfrac{\mathrm{d}I_L}{\mathrm{d}t}=(k-1)R_1 I_L-V_{C1}-V_{C2} \\ C_2\dfrac{\mathrm{d}V_{C2}}{\mathrm{d}t}=\dfrac{V_b}{R_4}+I_L-I_s\left(\exp\left(\dfrac{V_{C2}}{V_0}\right)-1\right) \end{cases} \tag{3.12b}$$

In the coming sections, dynamic analysis of Vilnius system will be done based on Eq.(3.12a). Eq.(3.12b) is the one used by the researchers until now. Resistor R_1 is going to be used as bifurcation parameter. In our dynamics study, we are going to consider $R_3=R_2$.

4. Stability Analysis

The first step for the analysis of the Vilnius dynamics is to study the stability of its equilibrium point (x_0, y_0, z_0) through Eq.(3.12a), by setting it equal to zero and obtain $y=y_0=0$, $x=x_0=z_0$ where z_0 is the solution of Eq.(4.1) which is nontrivial if a_1 is different of 0.

$$u-a_1 z_0-c\left(\mathrm{e}^{z_0}-1\right)=0 \tag{4.1}$$

The stability of the given equilibrium point can be studied by using the eigenvalues equation

$$\lambda^3+\lambda^2\left(a_1-a+c\mathrm{e}^{z_0}\right)-\lambda\left(aa_1+ac\mathrm{e}^{z_0}+1\right)+a_1-c\mathrm{e}^{z_0}=0 \tag{4.2}$$

Limit-cycle oscillation might occur if the solutions of Eq. (4.2) are pure imaginary values $\lambda=\pm i\omega$, where ω is the frequency of the corresponding harmonic oscillation which satisfies the following equation

$$\omega^2\left(a_1+a+ce^{z_0}\right)-a_1+ce^{z_0}=0 \tag{4.3}$$

That allow to have the frequency expression as follows

$$\omega=\sqrt{\frac{ce^{z_0}-a_1}{a_1+a+ce^{z_0}}} \tag{4.4}$$

Based on Eq.(4.4) ω exist if only if $ce^{z_0}>a_1$, this means that $z_0\geq\ln\left(\frac{V_0}{R_4I_s}\right)$

$\Rightarrow V_{C2}>V_0\ln\left(\frac{V_0}{R_4I_s}\right)$.

5. Numerical Results

5.1. Time Response

$C_1=1\,\text{nF}$, $k=2$, $C_2=147\,\text{pF}$, $L=1\,\text{mH}$, $V_b=3\,\text{V}$, $R_4=20\,\text{k}\Omega$, $I_s=0.3\,\text{mA}$, $V_0=0.026\,\text{V}$, $R_2=R_3=1\,\text{k}\Omega$ are the values used for numerical and experimental studies. For each regime, the initial conditions are: $I_L=V_{C1}=V_{C2}=0.0$.

The results of numerical simulation were obtained using python's odeint solver with a step size of 0.02 for the time response and the phase portrait. Regarding the bifurcation diagram, we used a fourth-order Runge-Kutta algorithm. The transient regime was eliminated by considering the minimun time equal to 0.01second to search for lacals maximun.

(**Figures 2-4**) are time reponse of the system based on the proposed model and the common used model which show that depending on the values of R_1 the system can behave differently. We observe that the time response of the two models can be slightly different for $R_1=150\,\Omega$ (**Figure 2(a)**, **Figure 2(b)**). This difference becomes more pronounced for $R_1=250\,\Omega$; while the proposed model exhibits biperiodic oscillations (**Figure 4(a)**), the other model is already in a chaotic dynamic (**Figure 4(b)**).

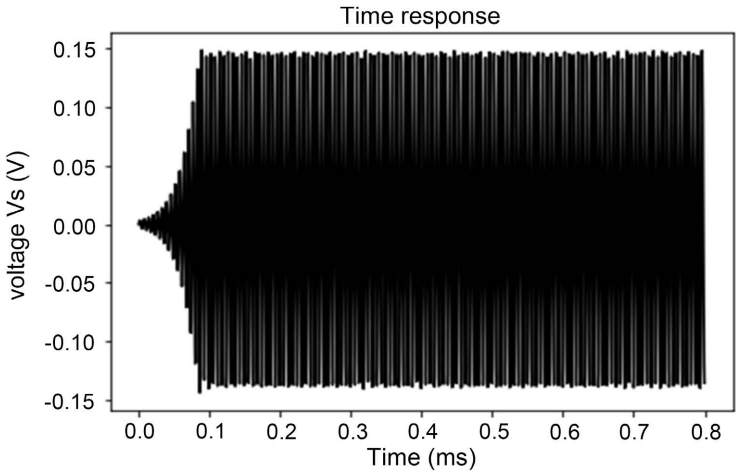

(a)

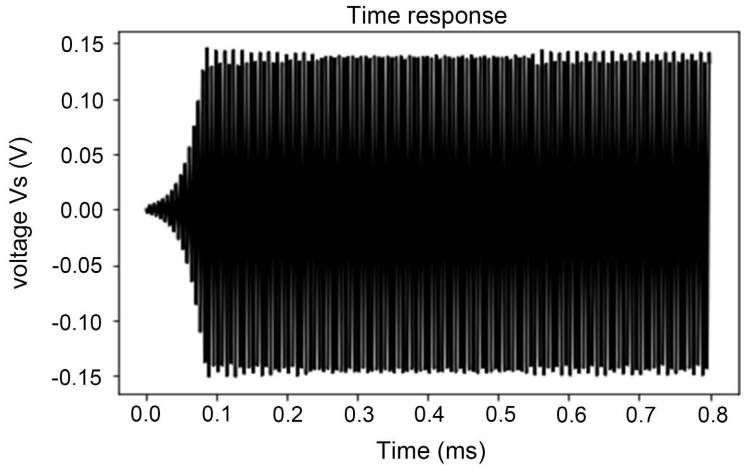

(b)

Figure 2. Time response for proposed model (a) and previous model (b) $R_1 = 150\,\Omega$.

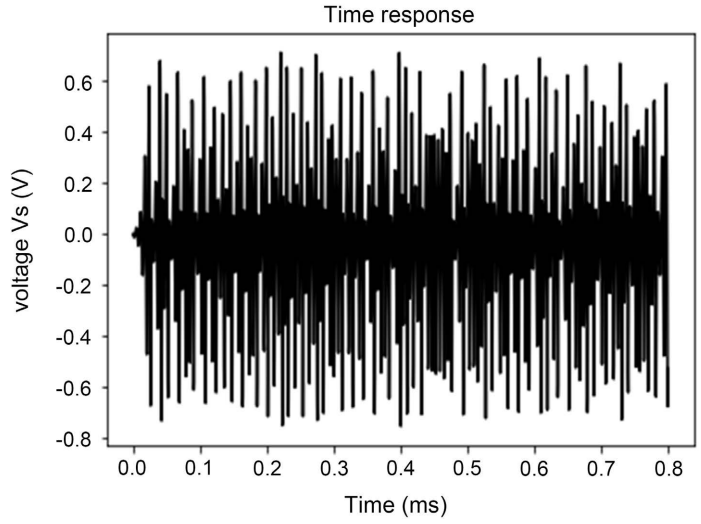

(a)

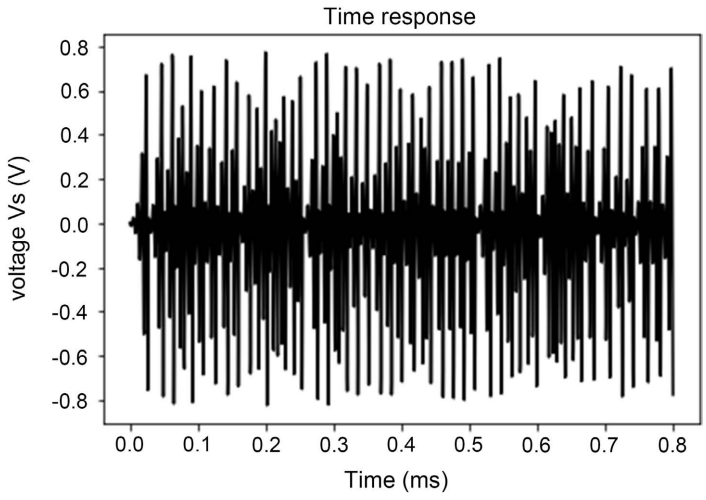

(b)

Figure 3. Time response for proposed model (a) and previous model (b) $R_1 = 150\,\Omega$.

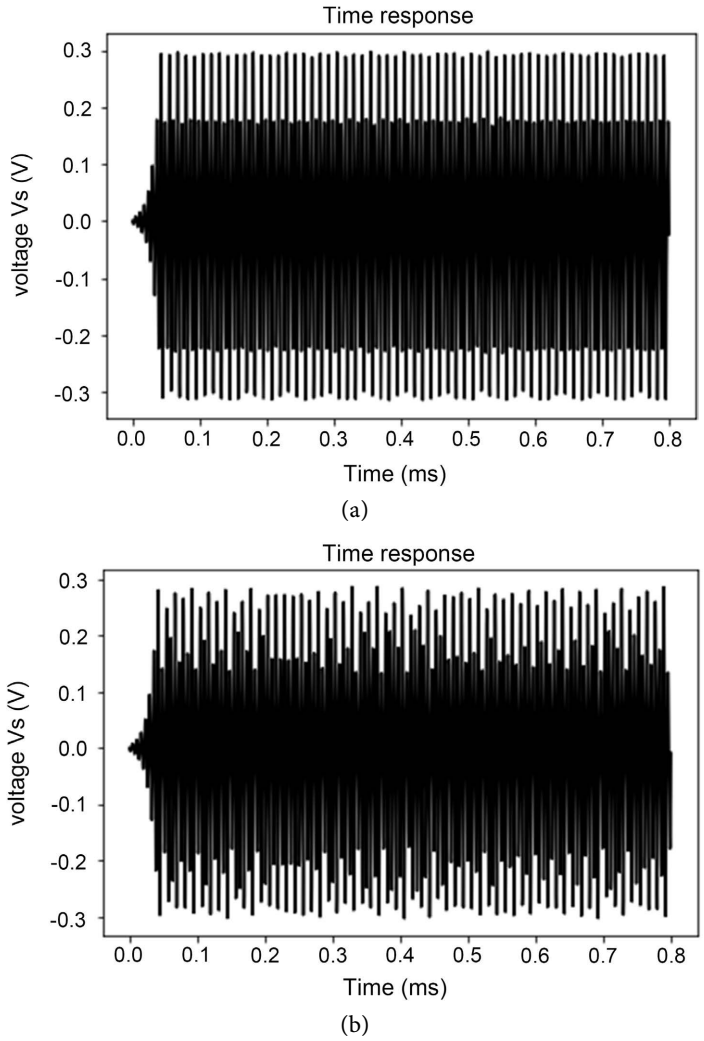

Figure 4. Time response for proposed model (a) and previous model (b) $R_1 = 150\,\Omega$.

5.2. Bifurcation Diagram and Lyapunov Exponents Curve

The largest Lyapunov exponents are compute following the formula:

$$\lambda = \lim_{\substack{t \to +\infty}} \frac{1}{t} \ln\left(\frac{|\delta x(t)|}{|\delta x(0)|}\right) \tag{4.5}$$

where $\delta x(t)$ is a small perturbation at time t and $\delta x(0)$ at $t = 0$.

Figures (**Figure 5**, **Figure 6**) are bifurcation diagram and Lyapunov exponent of Vilnius oscillator respectivly obtained with Eq.(3.12a) that we proposed. The bifurcation parameter here are the values of resistor R_1 which sets the voltage at the non-inverting terminal of the operational amplifier. Depending of the values of R_1 the system presents different types of dynamics. Thus, when $0 \le R_1 < 50\,\Omega$, the system converging toward a fixed point. In the same way, for $50 < R_1 < 175\,\Omega$, the system presents harmonic oscillations. For the values $175 < R_1 < 270\,\Omega$, we observe the multiperiodicity oscillations. When

$270 \le R_1 \le 920\,\Omega$, the system become chaotic with certain windows of stability and for the values of R_1 around 920Ω we can observe again the multiperiodic oscillations. Figure 6 represents the curve of the variations of the Lyapunov exponents of the Vilnius oscillator. This curve is in agreement with the bifurcation diagram. It is clearly observed that for $0 < R_1 < 270\,\Omega$ the system is stable. For R_1 slightly greater than 300Ω, the system become chaotic with a zone of stability observed for certain values of R_1. This result suggests that chaos appears early in the classical oscillator model and thus highlights the difference between this

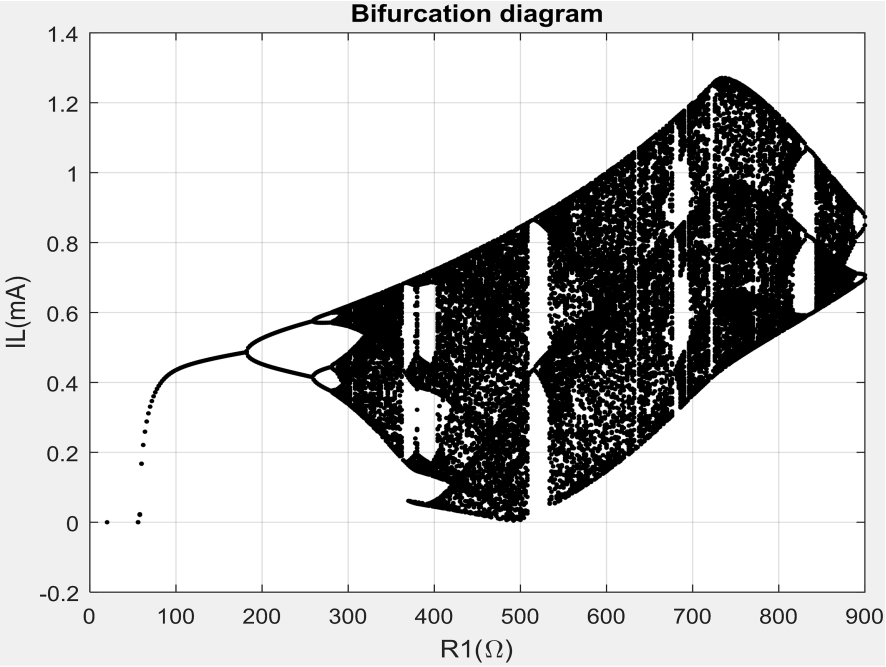

Figure 5. Bifurcation diagram for $0 \le R_1 \le 920\,\Omega$.

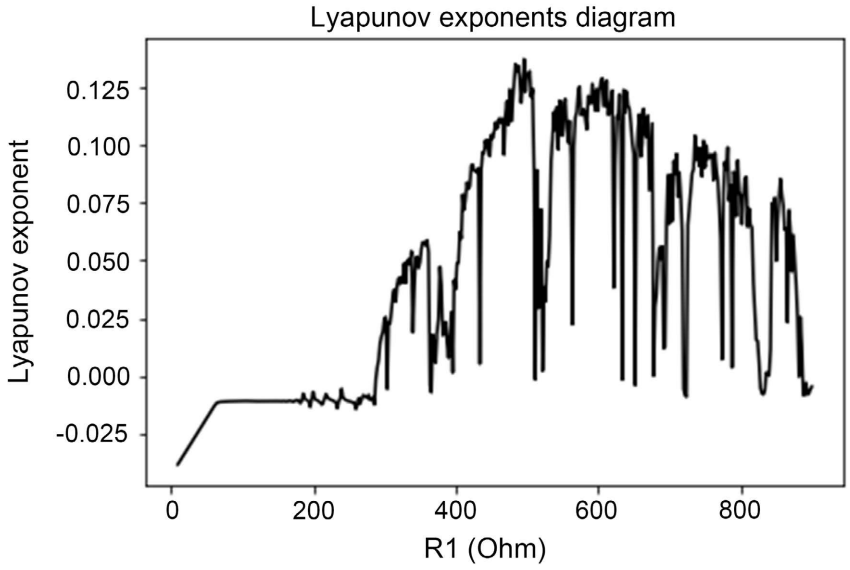

Figure 6. Largest Lyapunov exponents diagram for $0 \le R_1 \le 920\,\Omega$.

model and the one proposed. Figure 7 presents phase portrait of the circuit relative to voltage across the capacitor C_1 and the current flowing through them for $R_1 = 450\,\Omega$. It is clearly obseved that the dynamics of the circuit is chaotic as announced by the bifurcation diagram and the largest Lyapunov exponent curve. At this level, we can say that, with a given value of V_b, R_4, C_1, k, C_2, L_1 the dynamics of the Vilnius oscillator can exhibit different behaviors just by varying the values of the resistor R_1. This can therefore open a large possibility to apply effectively and efficiently the Vilnius oscillator in engineering by acting on the system at the appropriate point to have a usful signal.

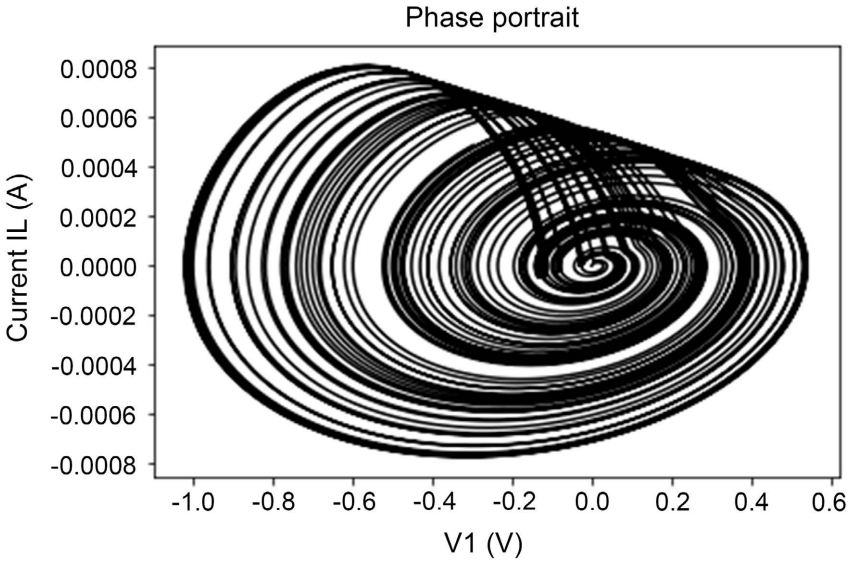

Figure 7. Phase portrait.

5.3. Frequency Responses

In this section, we always consider $R_3 = R_2$. The value of components used for the simulation are: $C_1 = 1\,\text{nF}$, $k = 2$, $C_2 = 147\,\text{pF}$, $L = 1\,\text{mH}$, $V_b = 3\,\text{V}$, $R_3 = R_2 = 1\,\text{k}\Omega$. The system of differential equations used for studying frequency response of the Vilnius oscillator is Eq. (5.1)

$$\begin{cases} \dfrac{\mathrm{d}x}{\mathrm{d}\tau} = y \\ \dfrac{\mathrm{d}y}{\mathrm{d}\tau} = ay - x - z \\ \dfrac{\mathrm{d}z}{\mathrm{d}\tau} = u\sin\left(\Omega_1\tau\right) - a_1 z + a_2 y - c\left(\exp\left(z\right) - 1\right) \end{cases} \tag{5.1}$$

Figure 8(a) and Figure 8(b) represent the frequency response of the system obtained respectively by the proposed model and the currently used model. We can observe a slight difference, but the maximum voltage across capacitor C_1 and the resonant frequency are approximataly the same. However, the resonance is sharper in the proposed model than the classical one.

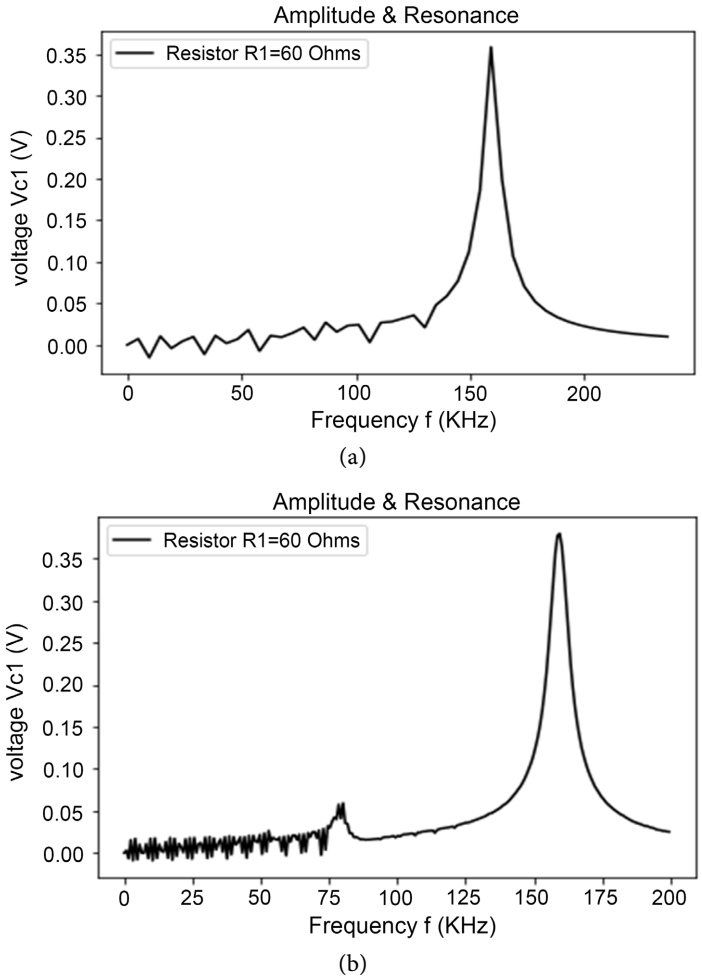

Figure 8. Frequency response for the proposed model (a) and previous model (b).

6. Expermental Results

Experimental setup consisting of an electronic circuit built with an operational amplifier (TL081), capacitors, coil, diode(1N4148), resistors and batteries whose values are contained in **Table 1**. Two batteries of 9 V are used to supply −9 and 9 V to the operational amplifier. Two other batteries of 1.5 V are use to power the circuit. The resistor R_1 is replaced by the potentiometer of 1k. The 47 pF and 100 pF capacitors were connected in parallel to obtain an equivalent of 147 pF.

The experimental activity consisted of two steps. In the First step, we studied the temporal response (**Figure 9**) of the system. To achieve that, the resistor R_1 connected between the non-inverting input of the operational amplifier and the ground was replaced by a potentiometer of 1 kΩ. By varying the potentiometer between its minimum and maximum values, different dynamics were observed on the oscilloscope screen. In the second step, the frequency response of the system was studied (**Figure 10**). This involved replacing the DC drive voltage with a 3 V AC voltage supplied by a low-frequency generator. We varied the generator frequency between 100 kHz and 200 kHz, which allowed us to obtain the values in **Table 2**.

Table 1. Values of capacitors, coil and resistances used in the electronic circuit.

Components	Values	Quantities
Coil	1 mH	01
Capacitor	1 nF	01
Capacitor	47 pF	01
Capacitor	100 pF	01
Resistor	1 k	02
Resistor	20 k	01
Potentiometer	1 k	01

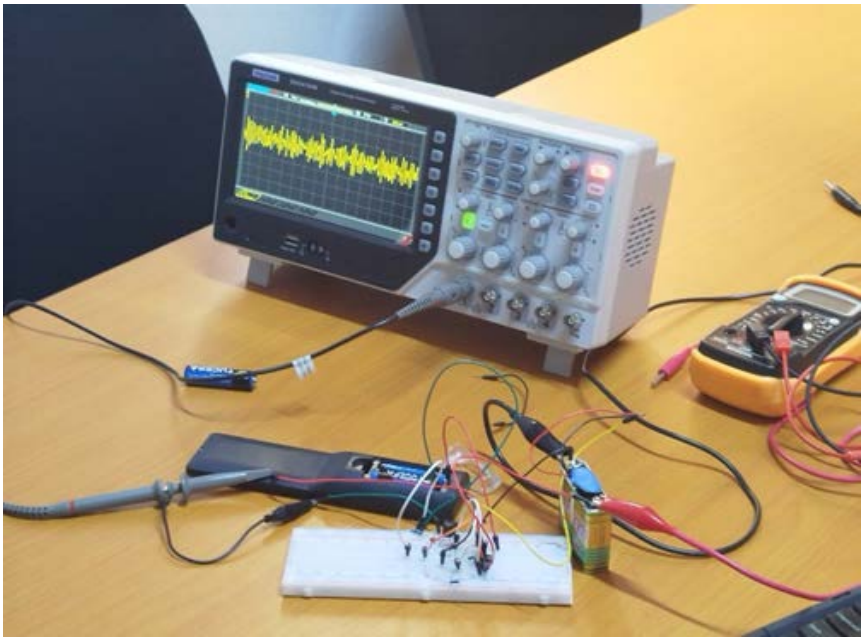

Figure 9. Experimental setup.

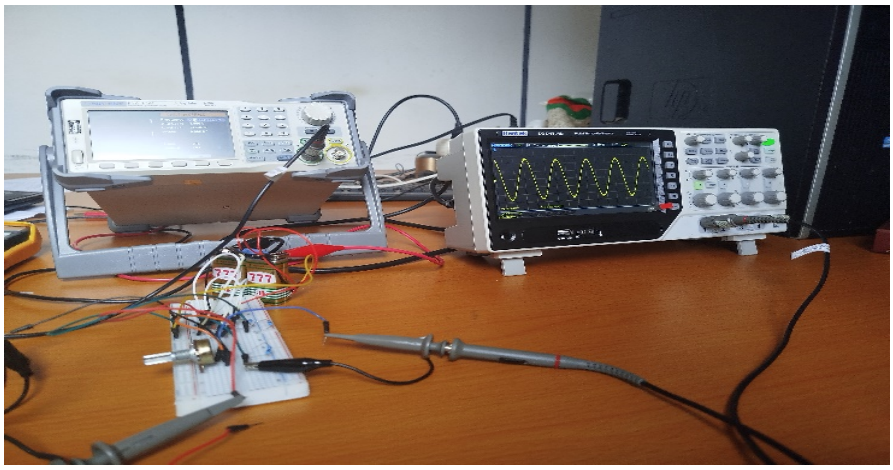

Figure 10. Experimental setup for frequency response.

Table 2. Experimental values of frequency and voltage.

f(Khz)	100	105	110	115	119	120
U(V)	0.43	0.51	0.64	0.96	1.84	2.6
125	130	135	140	145	150	155
2.8	0.92	0.53	0.36	0.244	0.192	0.156
160	165	170	175	180	185	190
0.13	0.11	0.096	0.088	0.07	0.062	0.05

We then plotted the corresponding curve in **Figure 11**. The experimental results obtained from the Vilnius eletronic oscillator show a qualitative agreement with the theoretical model as presented in **Figure 12** and **Figure 13** which are predicted by **Figure 2(a)**, **Figure 3(a)** and **Figure 7**. Theoretically, the model predicts a range of regimes, including sationary, harmonic oscillation, multiperiodic oscillation, and chaos as indicated by the bifurcation diagram and Lyapunov exponent curve (**Figure 5**, **Figure 6**). Experimentally, we observed stationary regime, harmonic oscillation (**Figure 12**), chaotic regime (**Figure 13**) and an additional regime that was not predicted by the theoretical model (**Figure 14**). This unexpected regime appears to be due to the saturation of the components used, particularly the operational amplifier TL081, which is not accounted in the theoretical model. Notably, the theoretical model predicts a chaotic regime with possible windows of stable oscillation for certain parameter values, whereas experimentally, we observed a distinct regime that does not fit into the predicted chaotic behavior zone. In the same way, harmonic oscillation that was not predicted theoretically in the absence of the driven voltage appears experimentally with oscillation frequency equal to 168.92 kHz (**Figure 15**).

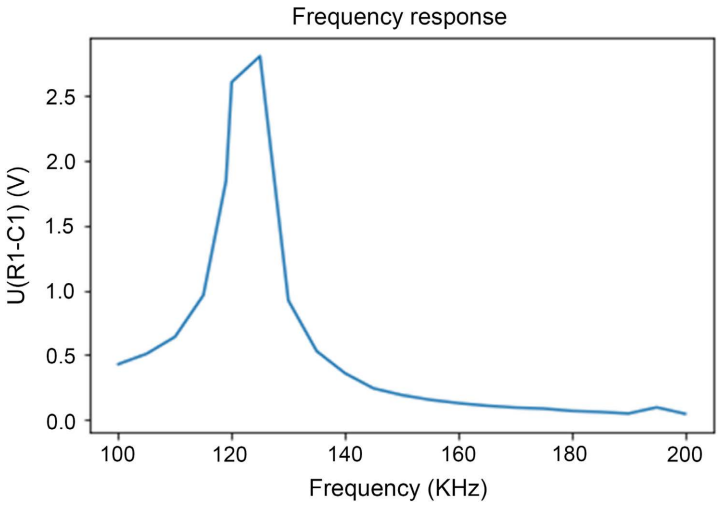

Figure 11. Experimental frequency response.

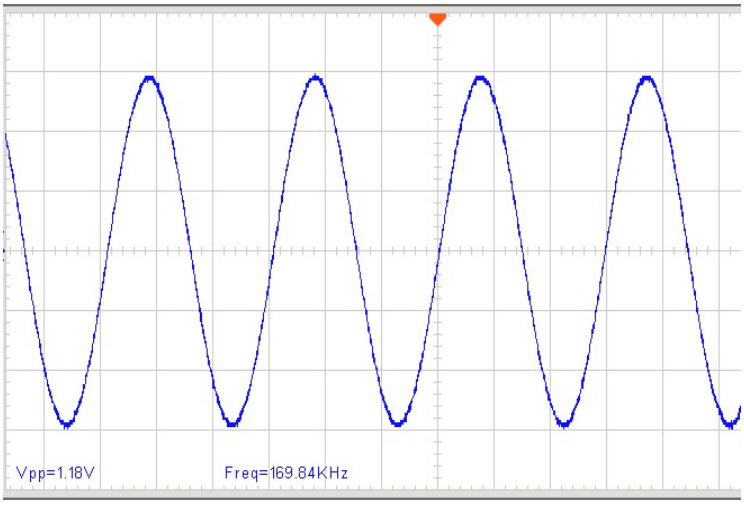

Figure 12. Experimental harmonic oscillation.

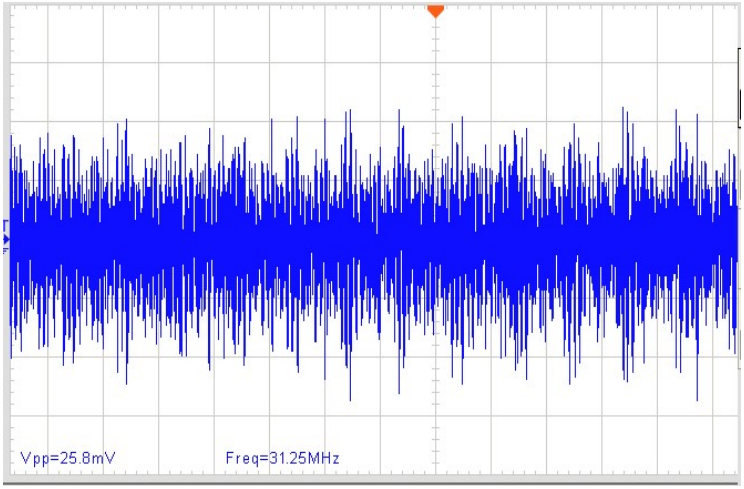

Figure 13. Experimental chaotic regime.

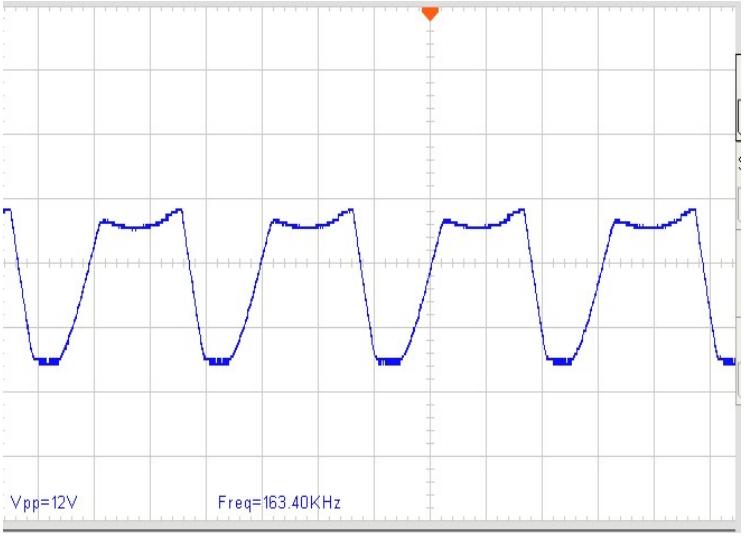

Figure 14. Experimental unpredicted regime.

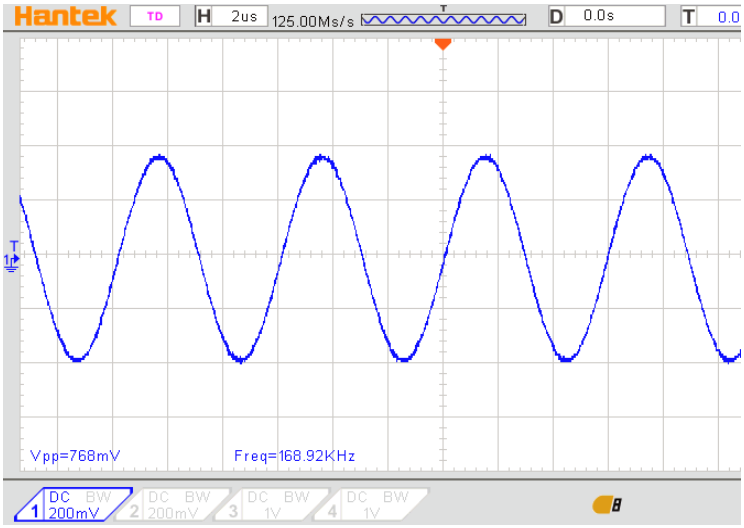

Figure 15. Free oscillation response.

Concerning the frequency response, the theoretical curve in **Figure 8** shows the resonance peak around 156 kHz whereas the experimental value is around 121 kHz (**Figure 11**). This difference between the theoretical and experimental resonance frequency values may be due to a modeling flaw, or even a possible interaction between the earth's magnetic field and that of the coil, thus modifying the inductance of the latter. These discrepancies highlight the limitations of the model and the importance of considering the nonlinear dynamics and component limitations such as construction uncertainties on the values of the resistances, the diode ideality factor in the system modelling. Despite these differences, the experimental results provide valuable insights into the behavior of Vilnius oscillation and demonstrate the richness of the system's dynamics. The experimental study also showed that the chaotic regime appears for R_1 values greater than 300 Ω, which is in agreement with the dynamic behavior of the proposed model. The lack of certain dynamics and additional regimes observed experimentally provides a new perspective on the system's behavior for further work which will consist of refining the theoretical model of the system.

7. Conclusion

In this paper, a new mathematical model of the Vilnius oscillator was derived from Kirchhoff's laws, by considering the excitation current as a variable. Theoretically, the time and frequency responses of the proposed model were determined, revealing a rich dynamic behavior as well as the system's natural frequency. Analysis of the bifurcation diagram and the Lyapunov exponent curve allowed us to identify different bifurcation phases, as well as chaotic and stable regions of the system, as a function of the values of its components and the control parameter. Subsequently, an experimental study with real components was conducted, demonstrating a qualitative agreement with the proposed theoretical model, compared to the previous one, particularly regarding the emergence of the chaotic regime as a

function of the control parameter values. This study also yielded a real resonance frequency slightly different from the theoretical frequency by approximately 36 kHz. The results of the proposed model showed that variations in the excitation current have a significant influence on the dynamic response of this oscillator and must be taken into account in future work. Finally, the experimental results revealed certain imperfections in the theoretical model, thus paving the way for its improvement and potential applications of the Vilnius oscillator in engineering.

Conflicts of Interest

The authors declare that they have no conflict of interest.

References

[1] Nana, B., Woafo, P. and Domngang, S. (2009) Chaotic Synchronization with Experimental Application to Secure Communications. *Communications in Nonlinear Science and Numerical Simulation*, **14**, 2266-2276. https://doi.org/10.1016/j.cnsns.2008.06.028

[2] Nana, B. and Woafo, P. (2015) Chaotic Masking of Communication in an Emitter-Relay-Receiver Electronic Setup. *Nonlinear Dynamics*, **82**, 899-908. https://doi.org/10.1007/s11071-015-2204-0

[3] Tcheutchoua Fossi, D.O. and Woafo, P. (2011) Dynamics of an Electromechanical System with Angular and Ferroresonant Nonlinearities. *Journal of Vibration and Acoustics*, **133**, Article ID: 061018. https://doi.org/10.1115/1.4004938

[4] Kocamaz, U.E. and Uyaroğlu, Y. (2014) Synchronization of Vilnius Chaotic Oscillators with Active and Passive Control. *Journal of Circuits, Systems and Computers*, **23**, Article ID: 1450103. https://doi.org/10.1142/s0218126614501035

[5] Ribordy, L. and Sands, T. (2023) Chaotic Van Der Pol Oscillator Control Algorithm Comparison. *Dynamics*, **3**, 202-213. https://doi.org/10.3390/dynamics3010012

[6] Tamaševičius, A., Mykolaitis, G., Pyragas, V. and Pyragas, K. (2004) A Simple Chaotic Oscillator for Educational Purposes. *European Journal of Physics*, **26**, 61-63. https://doi.org/10.1088/0143-0807/26/1/007

[7] Dmitrijs, P., Sergejs, T., Victor, C. and Ipatovs, A. (2022) Study of Nonlinear Dynamics of Vilnius Oscillator. In: *Nonlinear Dynamics and Applications*, Springer, 1219-1228.

[8] Babajans, R., Cirjulina, D., Capligins, F., Kolosovs, D., Grizans, J. and Litvinenko, A. (2023) Performance Analysis of Vilnius Chaos Oscillator-Based Digital Data Transmission Systems for IoT. *Electronics*, **12**, Article No. 709. https://doi.org/10.3390/electronics12030709

[9] Zhang, F., Gao, R., Huang, Z., Jiang, C., Chen, Y. and Zhang, H. (2022) Complex Modified Projective Difference Function Synchronization of Coupled Complex Chaotic Systems for Secure Communication in WSNs. *Mathematics*, **10**, Article No. 1202. https://doi.org/10.3390/math10071202

[10] Ipatovs, A., Victor, I.C., Pikulins, D., Tjukovs, S. and Litvinenko, A. (2023) Complete Bifurcation Analysis of the Vilnius Chaotic Oscillator. *Electronics*, **12**, Article No. 2861. https://doi.org/10.3390/electronics12132861